Acta Cryst E CRYSTALLOGRAPHIC COMMUNICATIONS

ISSN 2056-9890

Crystal structure of bis[(1-ammonio-1-phosphonoethyl)phosphonato]tetraaquacadmium dihydrate: a powder X-ray diffraction study

Mwaffak Rukiah[a]* and Thaer Assaad[b]

[a]Department of Chemistry, Atomic Energy Commission of Syria (AECS), PO Box 6091, Damascus, Syrian Arab Republic, and [b]Radioisotope Department, Atomic Energy Commission of Syria (AECS), PO Box 6091, Damascus, Syrian Arab Republic. *Correspondence e-mail: cscientific@aec.org.sy

Received 3 February 2015
Accepted 26 February 2015

Edited by V. V. Chernyshev, Moscow State University, Russia

Keywords: crystal structure; bisphosphonate complexes; complexes; cadmium; powder diffraction; octahedral coordination; zwitterion; hydrogen bonding

CCDC reference: 1051338
Supporting information: this article has supporting information at journals.iucr.org/e

In the title compound, $[CdL_2(H_2O)_4]\cdot 2H_2O$ [L = (1-ammonio-1-phosphonoethyl)phosphonate, $C_2H_8NO_6P_2^-$], the Cd^{II} ion is situated on an inversion centre being coordinated by four aqua molecules in the equatorial plane and two phosphonate O atoms from two deprotonated L ligands in the axial positions in a distorted octahedral geometry. The asymmetric unit contains one-half of the complex molecule and one lattice water molecule. The ligand L exists in a zwitterionic form, with a positive charge on the NH_3 group and a negative charge on the O atom of the non-coordinating phosphonate group, and with an intramolecular O—H···O interaction forming an $S(6)$ ring motif and two intramolecular N—H···O interactions each generating an $S(5)$ ring motif. In the crystal, N—H···O and O—H···O hydrogen bonds link the complex molecules into a three-dimensional network in which the voids of 38 Å^3 are filled with ordered lattice water molecules, which are also involved in O—H···O hydrogen bonding.

1. Chemical context

As a result of of their inhibitory effect on bone resorption, various types of bisphosphonates are used in the treatment of bone metastasis and several bone disorders such as Paget's disease, and for the prevention of osteoporosis in post-menopausal women (Shaw & Bishop, 2005). Drugs prepared on the basis of bisphosphonates are highly efficient as a regulator of calcium metabolism and the immune response; they are used as anti-neoplastic, anti-inflammatory and anti-viral agents, drugs with analgesic effect and, as a component of toothpastes, biphosphonates prevent the formation of tartar (Matkovskaya *et al.*, 2001). Organic diphosphonic acids are potentially very powerful chelating agents, used in metal extractions and have been tested by the pharmaceutical industry for use as efficient drugs preventing calcification and inhibiting bone resorption (Matczak-Jon & Videnova-Adrabińska, 2005). Diphosphonic acids and their metal complexes are used in the treatment of Paget's disease, osteoporosis and tumoral osteolysis (Szabo *et al.*, 2002). However, it is still not clearly understood why small structural modification of bisphosphonates may lead to extensive alterations in their physicochemical, biological and toxicological characteristics (Matczak-Jon & Videnova-Adrabińska, 2005). Therefore, the structure determination of bisphosphonates is very important in order to understand the influence of structural modifications on their complex-forming abilities and physiological activities.

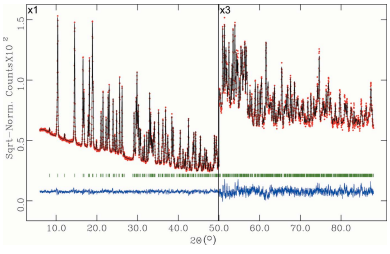

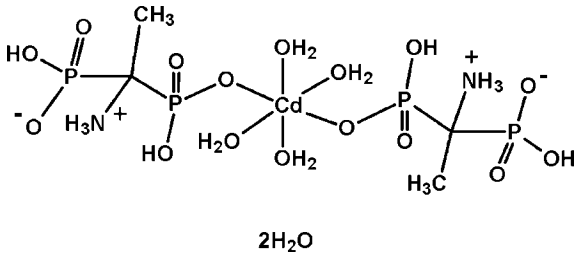

2. Structural commentary

The asymmetric unit of the title compound, (I) (Fig. 1), contains one half of the complex molecule $[CdL_2(H_2O)_4]$ [L = (1-ammonio-1-phosphonoethyl)phosphonate] and one lattice water molecule. All bond lengths and angles in (I) are normal and correspond to those observed in bisphosphonate complexes with transition metals (Shkol'nikova *et al.*, 1991; Sergienko *et al.*, 1997, 1999; Yin *et al.*, 2005; Li *et al.*, 2006; Li & Sun, 2007; Lin *et al.*, 2007; Xiang *et al.*, 2007; Dudko *et al.*, 2009, 2010; Bon *et al.*, 2010; Tsaryk *et al.*, 2010, 2011). The Cd^{II} atom occupies a special position on an inversion centre and shows a slightly distorted octahedral coordination environment formed by two phosphonic O atoms in *trans* positions and four aqua O atoms in the equatorial plane. The distorted octahedral coordination polyhedron is slightly compressed in the axial direction; the Cd1—O2 bond length is 0.1 Å shorter than the Cd1—O1*W* and Cd1—O2*W* bonds. The values of the axial O—Cd—O angles are in the range 80.1 (4)–99.9 (4)°, indicating a significant deviation from ideal values. The ligand L exists in a zwitterionic form, with a positive charge on the NH_3 group and a negative charge on the O atom of the non-coordinating phosphonate group, and with an intramolecular O—H···O interaction forming an $S(6)$ ring motif and two intramolecular N—H···O interactions each generating an $S(5)$ ring motif (Table 1).

3. Supramolecular features

The crystal packing is illustrated in Fig. 2 as a projection of the unit cell along the b axis. Intermolecular N—H···O and O—H···O hydrogen bonds (Table 1) link complex molecules into a three-dimensional network in which the voids of 38 Å^3 are filled with ordered lattice water molecules, which are also involved in O—H···O hydrogen bonding (Table 1 and Fig. 2).

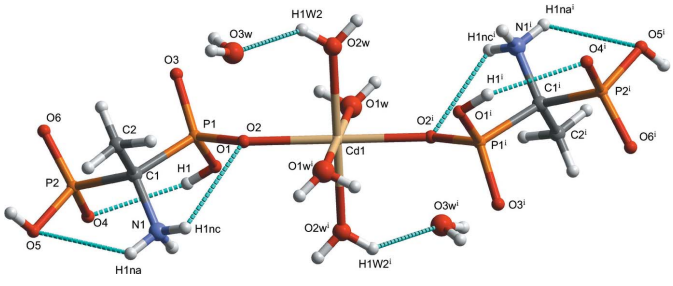

Figure 1
The molecular structure of (I), showing the atom-labelling scheme [symmetry code: (i) $-x+1, -y+1, -z+1$]. Displacement spheres are drawn at the 50% probability level. H atoms are represented as small spheres of arbitrary radii. Dotted lines denote hydrogen bonds.

Table 1
Hydrogen-bond geometry (Å, °).

D—H···A	D—H	H···A	D···A	D—H···A
O1—H1···O4	0.84	2.44	3.196 (13)	151
N1—H1NA···O6^{i}	0.87	2.07	2.828 (13)	146
N1—H1NB···O4^{ii}	0.88	2.16	2.872 (15)	137
N1—H1NC···O3^{i}	0.86	1.99	2.796 (14)	156
O1*W*—H1*W*1···O2*W*^{i}	0.82	2.39	2.987 (13)	131
O5—H5···O6^{iii}	0.84	1.79	2.551 (12)	150
O1*W*—H2*W*1···O3^{i}	0.82	1.96	2.758 (15)	162
O2*W*—H2*W*2···O4^{iv}	0.82	2.35	3.141 (15)	162
O3W—H1*W*3···O3W^{v}	0.82	2.56	3.346 (13)	160
O3W—H2*W*3···O3^{vi}	0.82	2.13	2.833 (14)	143

Symmetry codes: (i) $x, y+1, z$; (ii) $-x, -y+1, -z+1$; (iii) $-x, y+\frac{1}{2}, -z+\frac{3}{2}$; (iv) $x+1, y, z$; (v) $-x+1, y-\frac{1}{2}, -z+\frac{3}{2}$; (vi) $-x+1, y+\frac{1}{2}, -z+\frac{3}{2}$.

4. Synthesis and crystallization

All reactions and manipulations were carried out in air with reagent grade solvents. 1-Aminoethane-1,1-diyldiphosphonic acid was prepared according to the literature method of Rukiah & Assaad (2013). The title compound (I) was prepared by adding 10 ml of an 0.01 *M* $CdCl_2$ aqueous solution to 10 ml of a 0.02 *M* water solution of 1-aminoethane-1,1-diyldiphosphonic acid. A crude product was obtained after two weeks of slow evaporation of the resulted solution. It was further purified by recrystallization from ethanol and water (1:3 *v*/*v*) at 273 K to produce the title compound (I) (white powder; m.p. > 623 K) in 80% yield. The IR spectrum was recorded on a Jasco FT–IR 300E instrument and the ^{1}H and ^{13}C{^{1}H} NMR spectra were recorded on a Bruker Bio spin 400 spectrometer.

Spectroscopic data for (I):

^{1}H NMR (D_2O, p.p.m.): δ 1.67 (*t*, 3H, CH_3, J = 14 Hz). ^{13}C{^{1}H} NMR (D_2O, p.p.m.): δ 20.5 (1C; CH_3), 54.7 (1C; C—CH_3). ^{31}P{^{1}H} NMR (D_2O, p.p.m.): δ 13.61(2P; P—OH). IR (KBr, ν cm^{-1}): 3446.2 (NH_3), 2351.5 (POH), 1605.0 (O═P—O—H).

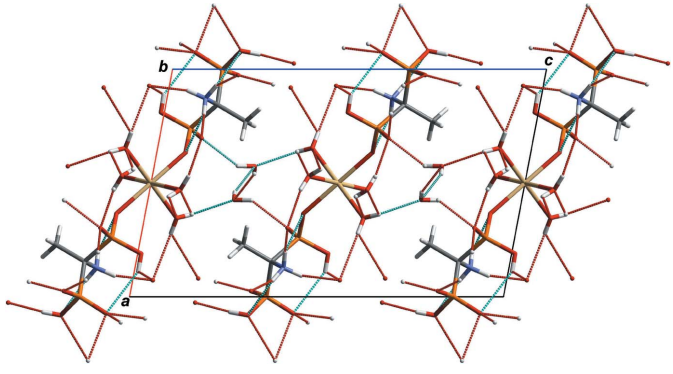

Figure 2
A portion of the crystal packing viewed down the b axis. Dashed lines denote hydrogen bonds.

Table 2
Experimental details.

Crystal data	
Chemical formula	$[Cd(C_2H_8NO_6P_2)_2(H_2O)_4]\cdot 2H_2O$
M_r	628.57
Crystal system, space group	Monoclinic, $P2_1/c$
Temperature (K)	298
a, b, c (Å)	10.69424 (12), 5.61453 (5), 17.2737 (2)
β (°)	100.7029 (8)
V (Å^3)	1019.12 (2)
Z	2
Radiation type	Cu $K\alpha_1$, λ = 1.5406 Å
μ (mm^{-1})	12.41
Specimen shape, size (mm)	Flat sheet, 8 × 8
Data collection	
Diffractometer	Stoe transmission STADI-P
Specimen mounting	Powder loaded into two Mylar foils
Data collection mode	Transmission
Scan method	Step
Absorption correction	For a cylinder mounted on the φ axis [*GSAS* (Larson & Von Dreele, 2004) absorption/surface roughness correction: function No. 4, flat-plate transmission absorption correction, terms = 0.75850]
T_{min}, T_{max}	0.195, 0.310
2θ values (°)	$2\theta_{min}$ = 6.00 $2\theta_{max}$ = 89.98 $2\theta_{step}$ = 0.02
Refinement	
R factors and goodness of fit	R_p = 0.029, R_{wp} = 0.039, R_{exp} = 0.025, $R(F^2)$ = 0.04534, χ^2 = 2.624
No. of data points	4100
No. of parameters	133
No. of restraints	4
H-atom treatment	H-atom parameters not refined

Computer programs: *WinXPOW* (Stoe & Cie, 1999), *GSAS* (Larson & Von Dreele, 2004), *EXPO2014* (Altomare *et al.*, 2013), *Mercury* (Macrae *et al.*, 2006) and *publCIF* (Westrip, 2010).

5. Refinement

Crystal data, data collection and structure refinement details are summarized in Table 2. Compound (I) has a tendency to crystallize in the form of a very fine white powder. Since no single crystals of sufficient size and quality could be obtained, a crystal structure determination from laboratory powder X-ray diffraction data was performed. The powder sample was ground slightly in a mortar, loaded into two Mylar foils and fixed onto the sample holder with a mask of suitable internal diameter (8.0 mm). The powder X-ray diffraction data were collected at room temperature with a STOE transmission STADI-P diffractometer using $CuK_{\alpha 1}$ radiation (λ= 1.54060 Å) selected with an incident-beam curved-crystal Ge(111) monochromator with a linear position-sensitive detector (PSD). The pattern was scanned over the angular range 6.0–90.0° (2θ). For pattern indexing, extraction of the peak positions was carried out with the program *WinPLOTR* (Roisnel & Rodríguez-Carvajal, 2001). Pattern indexing was performed with the program *DICVOL4.0* (Boultif & Louër, 2004). The first 20 intense peaks of the powder pattern were indexed completely on the basis of a monoclinic cell. The figures of merit (de Wolff *et al.*, 1968; Smith & Snyder, 1979) are sufficiently acceptable to support the obtained indexing results [$M(20)$ = 37.1, $F(20)$ = 78.5(0.0061, 42)]. The best estimated monoclinic space group was $P2_1/c$.

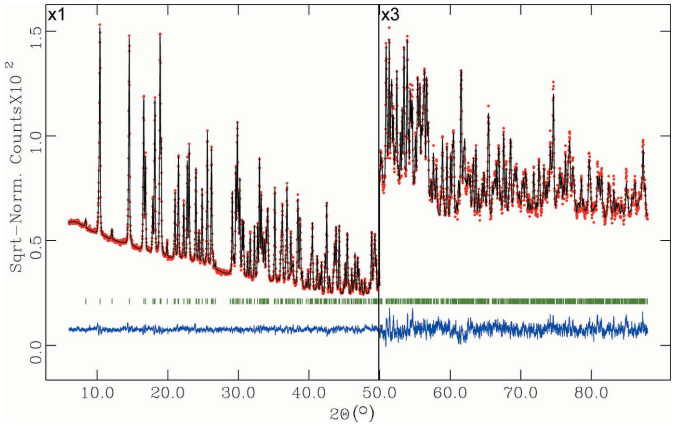

Figure 3
The final Rietveld plot for (I). Experimental intensities are indicated by dots, and the best-fit calculated (upper trace) and difference (lower trace) patterns are shown as solid lines. The vertical bars indicate the calculated positions of the Bragg peaks.

The powder pattern was subsequently refined with cell and resolution constraints (Le Bail *et al.*, 1988) using the profile-matching option of the program *FULLPROF* (Rodríguez-Carvajal, 2001). The number of molecules per unit cell was estimated to be Z = 2. The initial crystal structure was determined by direct methods using the program *EXPO2014* (Altomare *et al.*, 2013). The model found by this program was introduced into the program *GSAS* (Larson & Von Dreele, 2004) implemented in *EXPGUI* (Toby, 2001) for Rietveld refinement. The background was refined using a shifted Chebyshev polynomial with 20 coefficients. The effect of the asymmetry of the low-order peaks was corrected using a pseudo-Voigt description of the peak shape (Thompson *et al.*, 1987), angle-dependent asymmetry with axial divergence (Finger *et al.*, 1994) and microstrain broadening (Stephens, 1999). Two asymmetry parameters of this function, S/L and D/L, were both fixed at 0.0225 during this refinement. Intensities were corrected for absorption effects with a function for a plate sample in transmission geometry with $\mu\cdot d$ value of 0.7585 (μ is the absorption coefficient and d is the sample thickness). These $\mu\cdot d$ values were determined experimentally. The preferred orientation was modelled with 12 coefficients using a spherical harmonics correction (Von Dreele, 1997) of intensities. The use of the preferred orientation correction leads to a better molecular geometry with better agreement factors. The value of obtained median texture index (1.0654) and the agreement factors in the refinement without texture correction (R_p = 0.053, R_{wp} = 0.073, R_{exp} = 0.025, $R(F^2)$ = 0.011009 and χ^2 = 8.940) indicate that the preferred orientation improvement of the refinement is considerable.

Before the final refinement, the H atoms of the CH_3 and NH_3 groups were introduced on the basis of geometrical arguments. The hydroxy and water H atoms were located using the program *HYDROGEN* (Nardelli, 1999) implemented in *WinGX* (Farrugia, 2012). The coordinates of all H atoms were refined with very strict soft restraints on bond lengths and angle until a suitable geometry was obtained, after

that they were fixed in the final stage of the refinement. Four restraints for the central carbon atom (C—CH_3, C—NH_3 and two C—PO_3) on bond lengths were applied to normal values for these bonds. The final refinement cycles were performed varying isotropic displacement parameters for Cd and water O atoms, and fixed isotropic displacement parameters for P, C, N,O and H atoms. The final Rietveld plot is shown in Fig. 3.

Acknowledgements

We thank Professor I. Othman, Director General, Professor Z. Ajii, Head of the Chemistry Department, and Professor A. H. Al-Rayyes, Head of the Radioisotope Department, for their support of this work. We also thank Mr Emad Ghanem and Madame Najwa Karajoli for their kind assistance with the laboratory work.

References

Altomare, A., Cuocci, C., Giacovazzo, C., Moliterni, A., Rizzi, R., Corriero, N. & Falcicchio, A. (2013). *J. Appl. Cryst.* **46**, 1231–1235.
Bon, V. V., Dudko, A. V., Kozachkova, A. N., Pekhnyo, V. I. & Tsaryk, N. V. (2010). *Acta Cryst.* E**66**, m537–m538.
Boultif, A. & Louër, D. (2004). *J. Appl. Cryst.* **37**, 724–731.
Dudko, A., Bon, V., Kozachkova, A. & Pekhnyo, V. (2009). *Acta Cryst.* E**65**, m459.
Dudko, A., Bon, V., Kozachkova, A., Tsaryk, N. & Pekhnyo, V. (2010). *Acta Cryst.* E**66**, m170–m171.
Farrugia, L. J. (2012). *J. Appl. Cryst.* **45**, 849–854.
Finger, L. W., Cox, D. E. & Jephcoat, A. P. (1994). *J. Appl. Cryst.* **27**, 892–900.
Larson, A. C. & Von Dreele, R. B. (2004). *GSAS*. Report LAUR 86-748. Los Alamos National Laboratory, New Mexico, USA.
Le Bail, A., Duroy, H. & Fourquet, J. L. (1988). *Mater. Res. Bull.* **23**, 447–452.
Li, M., Chen, S., Xiang, J., He, H., Yuan, L. & Sun, J. (2006). *Cryst. Growth Des.* **6**, 1250–1252.
Li, M. & Sun, J.-T. (2007). *Acta Cryst.* E**63**, m1370–m1372.
Lin, L., Zhang, T., Fan, Y., Ding, D. & Hou, H. (2007). *J. Mol. Struct.* **837**, 107–117.
Macrae, C. F., Edgington, P. R., McCabe, P., Pidcock, E., Shields, G. P., Taylor, R., Towler, M. & van de Streek, J. (2006). *J. Appl. Cryst.* **39**, 453–457.
Matczak-Jon, E. & Videnova-Adrabińska, V. (2005). *Coord. Chem. Rev.* **249**, 2458–2488.
Matkovskaya, T. A., Popov, K. I. & Yuryeva, E. A. (2001). *Bisphosphonates. Properties, Structure and Application in Medicine*, p. 223. Moscow: Khimiya.
Nardelli, M. (1999). *J. Appl. Cryst.* **32**, 563–571.
Rodríguez-Carvajal, J. (2001). *Commission on Powder Diffraction (IUCr) Newsletter*, **26**, 12–19.
Roisnel, T. & Rodríguez-Carvajal, J. (2001). *Mater. Sci. Forum*, **378–381**, 118–123.
Rukiah, M. & Assaad, T. (2013). *Acta Cryst.* C**69**, 815–818.
Sergienko, V. S., Afonin, E. G. & Aleksandrov, G. G. (1999). *Koord. Khim.* **25**, 133–142.
Sergienko, V. S., Aleksandrov, G. G. & Afonin, E. G. (1997). *Zh. Neorg. Khim.* **42**, 1291–1296.
Shaw, N. J. & Bishop, N. J. (2005). *Arch. Dis. Child.* **90**, 494–499.
Shkol'nikova, L. M., Porai-Koshits, M. A., Fundamenskii, V. S., Poznyak, A. L. & Kalugina, E. V. (1991). *Koord. Khim.* **17**, 954–963.
Smith, G. S. & Snyder, R. L. (1979). *J. Appl. Cryst.* **12**, 60–65.
Stephens, P. W. (1999). *J. Appl. Cryst.* **32**, 281–289.
Stoe & Cie (1999). *WinXPOW*. Stoe & Cie, Darmstadt, Germany.
Szabo, Ch. M., Martin, M. B. & Oldfield, E. (2002). *J. Med. Chem.* **45**, 2894–2903.
Thompson, P., Cox, D. E. & Hastings, J. B. (1987). *J. Appl. Cryst.* **20**, 79–83.
Toby, B. H. (2001). *J. Appl. Cryst.* **34**, 210–213.
Tsaryk, N. V., Dudko, A. V., Kozachkova, A. N., Bon, V. V. & Pekhnyo, V. I. (2010). *Acta Cryst.* E**66**, m1533–m1534.
Tsaryk, N. V., Dudko, A. V., Kozachkova, A. N. & Pekhnyo, V. I. (2011). *Acta Cryst.* E**67**, o1651–o1652.
Von Dreele, R. B. (1997). *J. Appl. Cryst.* **30**, 517–525.
Westrip, S. P. (2010). *J. Appl. Cryst.* **43**, 920–925.
Wolff, P. M. de (1968). *J. Appl. Cryst.* **1**, 108–113.
Xiang, J., Li, M., Wu, S., Yuan, L.-J. & Sun, J. (2007). *J. Mol. Struct.* **826**, 143–149.
Yin, P., Wang, X.-C., Gao, S. & Zheng, L.-M. (2005). *J. Solid State Chem.* **178**, 1049–1053.

supporting information

Acta Cryst. (2015). E**71**, 342-345 [doi:10.1107/S2056989015004028]

Crystal structure of bis[(1-ammonio-1-phosphonoethyl)phosphonato]tetraaquacadmium dihydrate: a powder X-ray diffraction study

Mwaffak Rukiah and Thaer Assaad

Computing details

Data collection: *WinXPOW* (Stoe & Cie, 1999); cell refinement: *GSAS* (Larson & Von Dreele, 2004); data reduction: *WinXPOW* (Stoe & Cie, 1999); program(s) used to solve structure: *EXPO2014* (Altomare *et al.*, 2013); program(s) used to refine structure: *GSAS* (Larson & Von Dreele, 2004); molecular graphics: *Mercury* (Macrae *et al.*, 2006); software used to prepare material for publication: *publCIF* (Westrip, 2010).

Bis[(1-ammonio-1-phosphonoethyl)phosphonato]tetraaquacadmium dihydrate

Crystal data

$[Cd(C_2H_8NO_6P_2)_2(H_2O)_4]\cdot 2H_2O$
$M_r = 628.57$
Monoclinic, $P2_1/c$
Hall symbol: -P 2ybc
$a = 10.69424\ (12)$ Å
$b = 5.61453\ (5)$ Å
$c = 17.2737\ (2)$ Å
$\beta = 100.7029\ (8)°$
$V = 1019.12\ (2)$ Å^3
$Z = 2$
$F(000) = 636$
$D_x = 2.048$ Mg m^{-3}
Cu $K\alpha_1$ radiation, $\lambda = 1.5406$ Å
$\mu = 12.41$ mm^{-1}
$T = 298$ K
Particle morphology: fine powder
white
flat_sheet, 8 × 8 mm

Data collection

Stoe transmission STADI-P diffractometer
Radiation source: sealed X-ray tube
Ge 111 monochromator
Specimen mounting: Powder loaded into two Mylar foils
Data collection mode: transmission
Scan method: step
Absorption correction: for a cylinder mounted on the φ axis [GSAS (Larson & Von Dreele, 2004) absorption/surface roughness correction: function No. 4, flat-plate transmission absorption correction, terms = 0.75850]
$T_{min} = 0.195$, $T_{max} = 0.310$
$2\theta_{min} = 6.00°$, $2\theta_{max} = 89.98°$, $2\theta_{step} = 0.02°$

Refinement

Refinement on I_{net}
Least-squares matrix: full
R_p = 0.029
R_{wp} = 0.039
R_{exp} = 0.025
$R(F^2)$ = 0.04534
4100 data points

Profile function: CW Profile function number 4 with 21 terms Pseudovoigt profile coefficients as parameterized in (Thompson *et al.*, 1987). Asymmetry correction of (Finger *et al.*, 1994). Microstrain broadening by (Stephens, 1999). #1(GU) = 0.000 #2(GV) = 0.000 #3(GW) = 7.136 #4(GP) = 0.000 #5(LX) = 2.421 #6(ptec) = 0.11 #7(trns) = 0.00 #8(shft) = 0.0000 #9(sfec) = 0.00 #10(S/L) = 0.0225 #11(H/L) = 0.0225 #12(eta) = 0.6026 #13(S400) = 1.2E-02 #14(S040) = 1.0E-01 #15(S004) = 1.2E-03 #16(S220) = 3.3E-02 #17(S202) = 6.7E-03 #18(S022) = 1.7E-02 #19(S301) = 1.1E-02 #20(S103) = 2.3E-03 #21(S121) = 1.5E-02 Peak tails are ignored where the intensity is below 0.0010 times the peak Aniso. broadening axis 0.0 0.0 1.0
133 parameters
4 restraints
H-atom parameters not refined
Weighting scheme based on measured s.u.'s
$(\Delta/\sigma)_{max}$ = 0.03
Background function: GSAS Background function number 1 with 20 terms. Shifted Chebyshev function of 1st kind 1: 1216.00 2: -1325.95 3: 695.908 4: -224.478 5: 51.5854 6: -12.9254 7: 7.98937 8: -13.4593 9: 4.35490 10: 32.6578 11: -32.8988 12: -6.52632 13: -18.8133 14: 23.4504 15: -2.70081 16: -0.874623 17: -28.0163 18: 27.3423 19: 2.28961 20: -11.2631

Fractional atomic coordinates and isotropic or equivalent isotropic displacement parameters (Å²)

	x	*y*	*z*	U_{iso}*/U_{eq}
C1	0.1555 (5)	0.3764 (12)	0.6381 (5)	0.015*
C2	0.2285 (11)	0.4133 (17)	0.7222 (5)	0.015*
H2a	0.17609	0.50488	0.75213	0.02*
H2b	0.3063	0.50177	0.72104	0.02*
H2c	0.24919	0.26144	0.74755	0.02*
N1	0.1274 (11)	0.6170 (16)	0.6028 (7)	0.02*
H1na	0.07228	0.68814	0.62561	0.025*
H1nb	0.09382	0.59823	0.55236	0.025*
H1nc	0.19624	0.69829	0.60678	0.025*
P1	0.2594 (5)	0.2361 (7)	0.5774 (3)	0.01*
O1	0.1897 (8)	0.2047 (13)	0.4907 (6)	0.01*
H1	0.11151	0.1887	0.48952	0.015*
O2	0.3659 (9)	0.4155 (15)	0.5771 (6)	0.01*
O3	0.3024 (8)	−0.0094 (16)	0.6124 (6)	0.01*
P2	0.0019 (4)	0.2252 (6)	0.6342 (3)	0.01*
O4	−0.0728 (9)	0.1904 (14)	0.5539 (6)	0.01*
O5	−0.0807 (8)	0.4058 (11)	0.6745 (5)	0.01*

H5	−0.06622	0.38276	0.7235	0.03*
O6	0.0255 (7)	−0.0022 (16)	0.6785 (5)	0.01*
Cd1	0.5	0.5	0.5	0.0093 (7)*
O1W	0.5302 (11)	0.8211 (15)	0.5815 (7)	0.029 (4)*
H1W1	0.56	0.91732	0.55443	0.03*
H2W1	0.47216	0.89419	0.59649	0.03*
O2W	0.6537 (10)	0.2995 (14)	0.5866 (6)	0.020 (3)*
H1W2	0.63758	0.22791	0.62489	0.03*
H2W2	0.72024	0.23865	0.57871	0.03*
O3w	0.5739 (11)	0.3949 (14)	0.7310 (6)	0.028 (3)*
H1W3	0.54032	0.26314	0.72841	0.03*
H2W3	0.5752	0.43812	0.77663	0.03*

Geometric parameters (Å, º)

C1—C2	1.530 (12)	P2—O5	1.588 (7)
C1—N1	1.490 (12)	P2—O6	1.486 (9)
C1—P1	1.840 (9)	O5—H5	0.842
C1—P2	1.839 (7)	Cd1—O2	2.183 (8)
C2—H2a	0.976	Cd1—O2^{i}	2.183 (8)
C2—H2b	0.972	Cd1—O1W	2.274 (9)
C2—H2c	0.965	Cd1—O1W^{i}	2.274 (9)
N1—H1na	0.865	Cd1—O2W	2.300 (10)
N1—H1nb	0.885	Cd1—O2W^{i}	2.300 (10)
N1—H1nc	0.858	O1W—H1W1	0.817
P1—O1	1.555 (11)	O1W—H2W1	0.824
P1—O2	1.521 (9)	O2W—H1W2	0.820
P1—O3	1.541 (9)	O2W—H2W2	0.823
O1—H1	0.838	O3w—H1W3	0.820
P2—O4	1.480 (10)	O3w—H2W3	0.823
C2—C1—N1	107.2 (7)	C1—P2—O6	108.2 (5)
C2—C1—P1	110.1 (6)	O4—P2—O5	104.3 (5)
C2—C1—P2	113.1 (7)	O4—P2—O6	112.3 (6)
N1—C1—P1	104.6 (5)	O5—P2—O6	112.2 (5)
N1—C1—P2	107.0 (6)	P2—O5—H5	109.2
P1—C1—P2	114.3 (4)	O2—Cd1—O2^{i}	180.0
C1—C2—H2a	109.4	O2—Cd1—O1W	80.1 (4)
C1—C2—H2b	109.6	O2—Cd1—O1W^{i}	99.9 (4)
C1—C2—H2c	110.1	O2—Cd1—O2W	88.2 (3)
H2a—C2—H2b	108.6	O2—Cd1—O2W^{i}	91.8 (3)
H2a—C2—H2c	109.4	O2^{i}—Cd1—O1W	99.9 (4)
H2b—C2—H2c	109.7	O2^{i}—Cd1—O1W^{i}	80.1 (4)
C1—N1—H1na	109.5	O2^{i}—Cd1—O2W	91.8 (3)
C1—N1—H1nb	108.0	O2^{i}—Cd1—O2W^{i}	88.2 (3)
C1—N1—H1nc	110.1	O1W—Cd1—O1W^{i}	180.0
H1na—N1—H1nb	108.5	O1W—Cd1—O2W	89.0 (4)
H1na—N1—H1nc	111.4	O1W—Cd1—O2W^{i}	91.0 (4)

H1nb—N1—H1nc	109.1	O1W^{i}—Cd1—O2W	91.0 (4)
C1—P1—O1	111.5 (6)	O1W^{i}—Cd1—O2W^{i}	89.0 (4)
C1—P1—O2	104.5 (5)	O2W—Cd1—O2W^{i}	180.0
C1—P1—O3	109.1 (4)	Cd1—O1W—H1W1	101.2
O1—P1—O2	107.2 (5)	Cd1—O1W—H2W1	124.1
O1—P1—O3	109.4 (5)	H1W1—O1W—H2W1	104.3
O2—P1—O3	115.1 (6)	Cd1—O2W—H1W2	122.2
P1—O1—H1	109.4	Cd1—O2W—H2W2	129.1
P1—O2—Cd1	136.4 (6)	H1W2—O2W—H2W2	104.3
C1—P2—O4	114.8 (5)	H1W3—O3w—H2W3	104.3
C1—P2—O5	104.8 (4)		

O1W—Cd1—O2—P1	168.8 (9)	O1—P1—C1—C2	−177.9 (6)
O2W—Cd1—O2—P1	−101.9 (8)	O2—P1—C1—C2	−62.3 (7)
O1W^{i}—Cd1—O2—P1	−11.2 (9)	O3—P1—C1—C2	61.3 (7)
O2W^{i}—Cd1—O2—P1	78.1 (8)	O4—P2—C1—P1	−54.2 (6)
O3—P1—O2—Cd1	84.9 (9)	O5—P2—C1—P1	−168.0 (5)
C1—P1—O2—Cd1	−155.4 (7)	O6—P2—C1—P1	72.1 (6)
O1—P1—O2—Cd1	−37.0 (9)	O4—P2—C1—N1	61.1 (8)
O1—P1—C1—P2	53.6 (6)	O5—P2—C1—N1	−52.7 (8)
O2—P1—C1—P2	169.2 (5)	O6—P2—C1—N1	−172.6 (7)
O3—P1—C1—P2	−67.2 (6)	O4—P2—C1—C2	178.9 (6)
O1—P1—C1—N1	−63.1 (7)	O5—P2—C1—C2	65.0 (7)
O2—P1—C1—N1	52.5 (8)	O6—P2—C1—C2	−54.9 (7)
O3—P1—C1—N1	176.1 (7)		

Symmetry code: (i) −*x*+1, −*y*+1, −*z*+1.

Hydrogen-bond geometry (Å, º)

D—H···*A*	*D*—H	H···*A*	*D*···*A*	*D*—H···*A*
O1—H1···O4	0.84	2.44	3.196 (13)	151
O1—H1···O4^{ii}	0.84	2.27	2.592 (12)	103
N1—H1NA···O5	0.87	2.53	2.986 (14)	114
N1—H1NA···O6^{iii}	0.87	2.07	2.828 (13)	146
N1—H1NB···O4^{iv}	0.88	2.16	2.872 (15)	137
N1—H1NC···O2	0.86	2.53	2.899 (15)	107
N1—H1NC···O3^{iii}	0.86	1.99	2.796 (14)	156
O1*W*—H1*W*1···O2*W*^{iii}	0.82	2.39	2.987 (13)	131
O5—H5···O6^{v}	0.84	1.79	2.551 (12)	150
O1*W*—H2*W*1···O3^{iii}	0.82	1.96	2.758 (15)	162
O2*W*—H1*W*2···O3W	0.82	2.27	2.833 (15)	126
O2*W*—H2*W*2···O4^{vi}	0.82	2.35	3.141 (15)	162
O3W—H1*W*3···O3W^{vii}	0.82	2.56	3.346 (13)	160
O3W—H2*W*3···O3^{viii}	0.82	2.13	2.833 (14)	143

Symmetry codes: (ii) −*x*, −*y*, −*z*+1; (iii) *x*, *y*+1, *z*; (iv) −*x*, −*y*+1, −*z*+1; (v) −*x*, *y*+1/2, −*z*+3/2; (vi) *x*+1, *y*, *z*; (vii) −*x*+1, *y*−1/2, −*z*+3/2; (viii) −*x*+1, *y*+1/2, −*z*+3/2.